



Proceeding Paper

Discovery of a Selective PI3K Inhibitor Through Structure-Based Docking and Multilevel In Silico Validation †

Manjiri Bharasakare *, Rahul D. Jawarkar *, Pravin N. Khatale and Pramod V. Burakle

Department of Pharmaceutical Chemistry, Dr Rajendra Gode Institute of Pharmacy, University Mardi Road, Ghatkheda, Amravati 444602, Maharashtra, India; email1@email.com (P.N.K.); email2@email.com (P.V.B.)

- * Correspondence: manjiribharasakare@gmail.com (M.B.); rdjawarkar@drgiop.ac.in (R.D.J.)
- [†] Presented at the 29th International Electronic Conference on Synthetic Organic Chemistry (ECSOC-29); Available online: https://sciforum.net/event/ecsoc-29.

Abstract

Phosphoinositide 3-kinase (PI3K) represents a pivotal therapeutic target implicated in cellular proliferation, metabolic processes, and oncogenic mechanisms. This research delineates a comprehensive in silico methodology aimed at identifying effective and pharmacokinetically favorable inhibitors of PI3K. Structure-based molecular docking was executed targeting the ATP-binding pocket of PI3K, revealing that the highest-ranked compound, MOL ID: 11325, demonstrated a significant binding affinity, reflected by a docking score of -8.558 kcal/mol. ADMET and SwissADME profiling confirmed that molecule 11325 is Lipinski-compliant, P-gp non-substrate, has a bioavailability score of 0.55, no PAINS or Brenk alerts, and a favorable synthetic accessibility (2.68), supporting its druglikeness and development potential. A 100 ns molecular dynamics simulation confirmed the stability of the PI3K-ligand complex, demonstrating minimal deviations in root mean square deviation (RMSD) and root mean square fluctuation (RMSF). The binding free energy, determined through the MMGBSA method, exhibited a favorable value (ΔG_{\perp} bind \approx -58.6 kcal/mol), thereby corroborating the ligand's affinity. The FEL analysis revealed distinct low-energy states, while the PCA indicated minimal structural fluctuations, confirming a stable and specific binding mode. Molecule 11325 was designated as a novel, druglike, and dynamically stable PI3K inhibitor by this integrated computational approach, indicating that it requires additional preclinical validation for therapeutic development.

Keywords: PI3K Inhibitor; molecular docking; SwissADME; FEL; MMGBSA; PCA

1. Introduction

Phosphoinositide 3-kinases (PI3Ks) are an important group of lipid kinases that add a phosphate group to the 3'-hydroxyl group of phosphatidylinositols [1]. This makes second messengers that are needed to control many cellular processes, such as growth, metabolism, movement, and survival. Receptor tyrosine kinases and -protein-coupled receptors turn on Class I PI3Ks [2,3]. Abnormal signaling in these pathways has been firmly associated with the onset of cancer, metabolic disorders, and immune system dysfunction. As a result, PI3K and its downstream effectors, such as AKT and mTOR, are recognized as critical components in cancer biology, making the PI3K/AKT/mTOR pathway one of the most thoroughly examined targets in the development of oncology therapies [4–6]. Genomic studies reveal that alterations such as mutations, amplifications, and

Chem. Proc. 2025, x, x https://doi.org/10.3390/xxxxx

dysregulation of PI3K isoforms are common in both solid tumors and hematologic malignancies. Mutations that activate the PIK3CA gene, which encodes the p110 α catalytic subunit, are frequently found in breast, colorectal, and endometrial cancers [7–9]. The PI3Kδ and PI3Kγ isoforms are crucial in B-cell malignancies and immune system disorders, underscoring the promise of isoform-selective inhibitors [10]. Despite this potential, the development of therapeutically effective PI3K inhibitors has faced considerable challenges, including dose-limiting toxicities, insufficient selectivity, and adaptive resistance mechanisms that hinder the durability of response [11,12]. Currently, several PI3K inhibitors have received regulatory approval, including idelalisib, which specifically targets PI3K5; copanlisib, a pan-PI3K inhibitor that is most effective against PI3K α/δ ; duvelisib; and alpelisib, recognized as the first selective PI3K α inhibitor approved for PIK3CA-mutated breast cancer [13]. Even though these drugs show that PI3K is a good target for treatment, clinical studies have shown that they have big problems with potency, isoform selectivity, tolerability, and pharmacokinetic properties [14,15]. The identified limitations underscore the ongoing necessity to identify novel scaffolds that exhibit improved binding selectivity and favorable drug-like properties. In the last twenty years, computational drug design has changed how we find kinase inhibitors. High-throughput screening is helpful, but it needs a lot of resources and is often limited by how much chemical space can be explored. In silico methods like molecular docking, molecular dynamics (MD), pharmacophore modeling, and free energy calculations, on the other hand, make it easier to look at ligandprotein interactions at the atomic level. This assists scientists in enhancing lead compounds [16,17]. Molecular docking is especially advantageous for PI3K due to the highly conserved ATP-binding cleft, which exhibits subtle isoform-specific variations in hydrophobic pockets and hinge-binding motifs that can be exploited for selectivity [16,18]. Later molecular dynamics simulations give us more information about conformational flexibility, ligand stability, and solvent interactions, which makes static docking predictions more accurate [19]. Free energy methods, including MM-GBSA [20] and thermodynamic integration, provide a quantitative evaluation of binding affinity. Principal component analysis (PCA) and free energy landscape (FEL) mapping, on the other hand, make it easier to understand conformational ensembles that are important for ligand recognition [21]. Recent publications have effectively utilized these integrated computational methodologies to discover novel scaffolds for PI3K and associated kinases. For example, small molecules with two hinge-binding hydrogen bonds and van der Waals interactions in hydrophobic subpockets have shown better binding affinity and selectivity. SwissADME and ADMET profiling techniques provide preliminary insights into the risks associated with pharmacokinetics and toxicity, thereby reducing the incidence of failures in lead optimization. There have been some improvements, but many modern PI3K inhibitors still have issues that make them hard to use in many clinical settings [22-28]. Interacting with other kinases that aren't the target can cause serious side effects, such as high blood sugar, stomach problems, and a weaker immune system. Resistance mechanisms, including pathway reactivation or compensatory signaling via parallel kinases, diminish long-term efficacy. So, next-generation inhibitors need to bind tightly, have good ADME properties, be less toxic, and only work on certain isoforms. A structure-guided approach makes these inhibitors better. For example, the right hinge-binding motifs, a good balance of polarity and lipophilicity, and a rigid scaffold are all important for success. Ligands that create stable hydrophobic interactions with essential residues (e.g., Trp812, Tyr867, Ile831/879/881 in $PI3K\alpha$) and transient, oriented hydrogen bonds with hinge residues like Val882 are especially interesting [14,29–32]. In kinase pharmacology, these motifs are clearly defined and are often associated with greater selectivity and enthalpic binding benefits [32]. This study uses a multilayer in silico pathway to find and confirm new PI3K inhibitors, which improves the existing framework. To target the ATP-binding pocket of PI3K, docking based on structure was used. The results show that there are ways to change the scaffold, such as making hinge-binding interactions better and making hydrophobic substituents longer, which is important for the strategic design of inhibitors that are important for health.

2. Methodology

2.1. Molecular Docking

Using AutoDock 4.2 [33,34], molecular docking was done to guess how ligands would fit into the ATP-binding site of Phosphoinositide 3-kinase (PI3K; PDB ID: 1E7U) [35]. We got the crystal structure from the RCSB Protein Data Bank and got it ready by taking out the crystallographic water molecules and co-crystallized ligands. Using AutoDock Tools (ADT), polar hydrogens were added, and Gasteiger charges were given. Before docking, the MMFF94 force field [36] was used to minimize the ligands (https://www.chemdiv.com/catalog/diversity-libraries/3d-diversity-natural-product-like-library/). The docking grid was $60 \times 60 \times 60$ Å with a 0.375 Å space between each point. It was centered on the ATP-binding cleft. The Lamarckian Genetic Algorithm (LGA) was used with 50 independent runs. Based on the docking score and interaction profile [37], the pose with the highest score was chosen. We used PyMOL and LigPlot+ to see how proteins and ligands interacted with each other.

2.2. Molecular Dynamics Simulation

We used the Desmond v6.3 module (Schrodinger, LLC) to run molecular dynamics (MD) simulations to see how stable docked complexes were. A TIP3P orthorhombic water box with a 10 Å buffer was used to solvate each protein–ligand system. To balance the charges, counterions were added, and 0.15 M NaCl was added to mimic normal body conditions. The OPLS_2005 force field was used to make the system as small as possible. After minimization, equilibration was performed under NVT (constant number, volume, temperature) and NPT (constant number, pressure, temperature) ensembles for 2 ns each [38–40]. Then, the Nose–Hoover thermostat and Martyna–Tobias–Klein barostat were used to run production simulations for 100 ns at 300 K and 1 atm. Desmond's analysis tools were used to figure out the Root Mean Square Deviation (RMSD), Root Mean Square Fluctuation (RMSF), Radius of Gyration (Rg), and hydrogen bond occupancy for the trajectory analyses [41–45].

2.3. MM-GBSA Binding Free Energy Calculations

The MM-GBSA (Molecular Mechanics/Generalized Born Surface Area) method in Schrödinger's Prime module was used to figure out the binding free energy. Every 10 ns, snapshots were taken from MD trajectories, and then energy minimization was done on them. The VSGB 2.0 solvation model and the OPLS_2005 force field were used. We used the following equation to figure out the binding free energy (ΔG _bind):

$$\Delta Gbind = Gcomplex - (Gprotein + Gligand) \ \Delta G_{bind} \ [46] = G_{complex} - (G_{protein} + G_{ligand}) \ \Delta Gbind = Gcomplex - (Gprotein + Gligand).$$

where GcomplexG_{complex} Gcomplex, GproteinG_{protein}Gprotein, and GligandG_{ligand}Gligand are the minimized free energies of the complex, protein, and ligand, respectively. Energy decomposition was conducted to assess the contributions from van der Waals, electrostatic, solvation, and lipophilic interactions [47,48].

2.4. Principal Component Analysis (PCA)

Principal Component Analysis (PCA) was employed to identify the predominant collective motions of the protein-ligand complexes during simulations. The trajectories were

aligned with the reference structure, and a covariance matrix of atomic positional fluctuations ($C\alpha$ atoms) was created. Eigenvectors and eigenvalues were computed, and the initial two principal components (PC1 and PC2) were examined. We plotted projections of MD snapshots along the PC1–PC2 axes to find conformational clusters and metastable states [49,50].

2.5. Free Energy Landscape (FEL)

The Free Energy Landscape (FEL) was created by projecting conformation ensembles onto the first two principal components (PC1 and PC2) from MD trajectories. We used the Boltzmann relation to find free energy (Δ G):

$$\Delta G(x,y) = -RT \ln P(x,y) \Delta G(x,y) = -RT \ln P(x,y) \Delta G(x,y) = -RT \ln P(x,y)$$

where P(x,y) is the probability distribution along PC1–PC2, R is the universal gas constant, and T is the temperature (300 K). Stable conformational states were linked to low-energy basins, while shallow local minima showed metastable states. GROMACS 2020.4 made the FEL plots, and OriginPro 2022 showed them [43,51,52].

3. Results and Discussion

3.1. Molecular Docking and MMGBSA Study

In the ATP-binding pocket of Phosphoinositide 3-kinase (PI3K; PDB: 1e7u), compound 11325 shows a well-structured and chemically compatible way to bind. The docking score of –8.558 kcal/mol supports this, as it shows a strong predicted affinity for a kinase active site of this size and hydrophobic nature. According to the contact map, a hydrophobic "support" made up of TRP812, ILE831, TYR867, ILE879, and ILE881 stabilizes the conformation at very short edge-to-edge distances (3.2–3.8 Å; specifically, TRP812 3.40 Å, ILE831 3.79 Å, TYR867 3.23 Å, ILE879 3.60 Å, and ILE881 3.69 Å). This lets the ligand's nonpolar scaffold make the most of van der Waals interactions and keep the pocket from getting too wet (see Table 1).

Table 1. Depiction of Docking interactions for the ligand 11325 with Phosphoinositide 3-kinase (PI3K) receptor (pdb: 1e7u).

1 812A TRP 3.40 14222 9843 2 831A ILE 3.79 14228 10125 3 867A TYR 3.23 14227 10733	Hydrophobic Interactions							
	1	812A		TRP	3.40	14222	9843	
3 867A TYR 3.23 14227 10733	2	831A		ILE	3.79	14228	10125	
	3	867A		TYR	3.23	14227	10733	
4 879A ILE 3.60 14233 10901	4	879A		ILE	3.60	14233	10901	
5 881A ILE 3.69 14218 10934	5	881A		ILE	3.69	14218	10934	
Hydrogen Bonds								
1 882A VAL 1.85 2.75 145.58 14221 [Nam] 10950 [O2]	1	882A V	1.85	2.75	145.58	14221 [Nam]	10950 [O2]	
2 882A VAL 1.98 2.98 172.45 10947 [Nam] 14212 [Nar]	2	882A V	AL 1.98	2.98	172.45	10947 [Nam]	14212 [Nar]	

10.1016/j.bmcl.2013.01.072 [53] The specified atom types include ligand Nam protein carbonyl O2 and ligand Heteroaromatic/Nam Nar ↔ carbonyl/amide protein. Make the case for traditional hinge-like hydrogen bonding, in which the ligand gives to and/or receives from the hinge residue's backbone. This interaction motif is recognized to substantially enhance kinase selectivity and enthalpic advantage. The geometry (sub-2.0 Å donor–acceptor separation and >145° angles) shows that there are strong, directional hydrogen bonds that can handle even small changes in the side chain. Two of these interactions help "pin" the ligand in a position where its hydrophobic surfaces line up with the nearby

nonpolar wall (TRP/TYR/ILE triad). This is why the docking score is so good (see Figure 1).

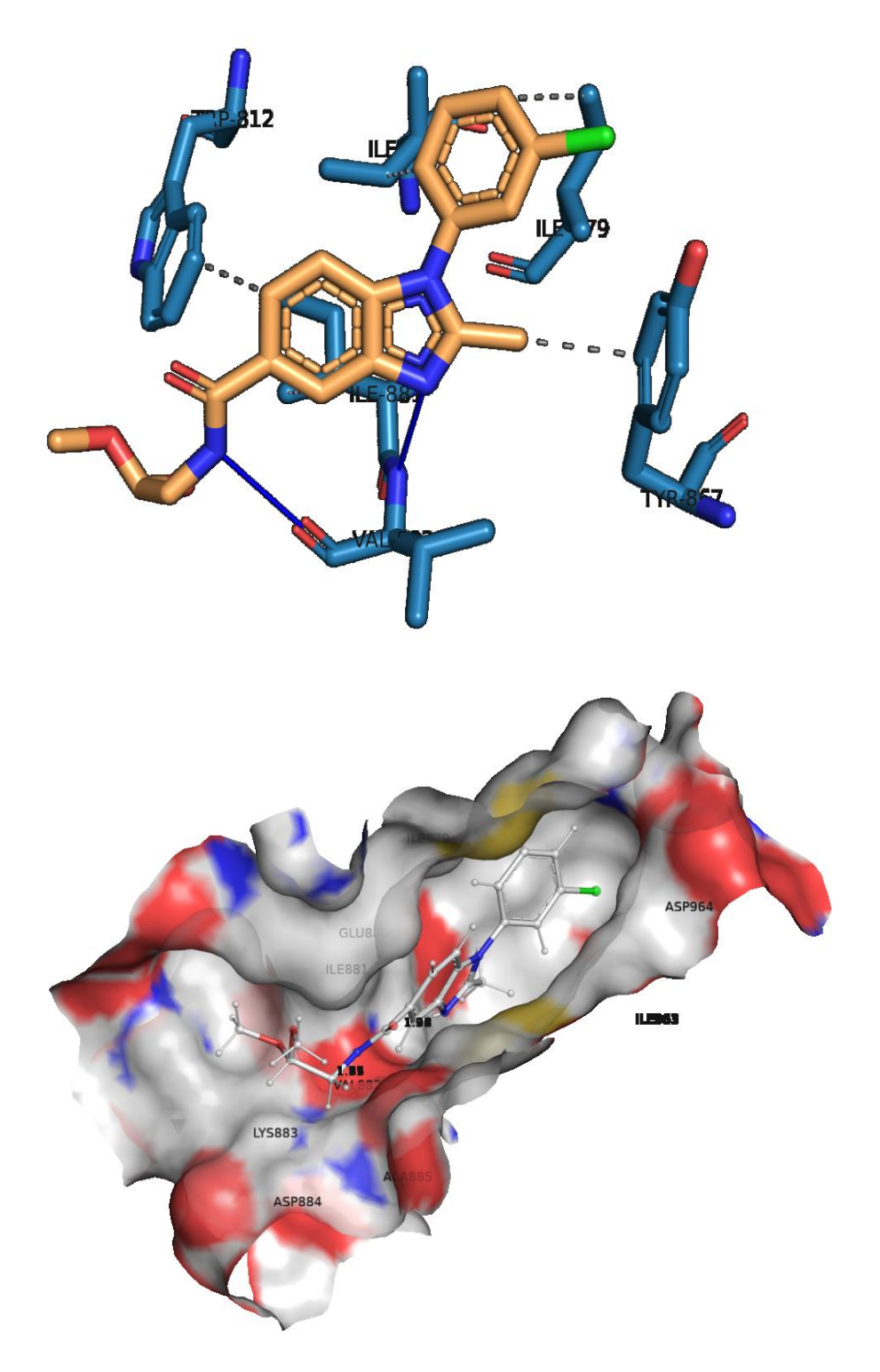


Figure 1. Portrayal of 3D and surface interactions of ligand 11325 with Phosphoinositide 3-kinase (PI3K) receptor (pdb: 1e7u).

This aligns with the anticipated outcomes of a conformation characterized by proximate hydrophobic interactions involving TRP812, TYR867, and multiple ILE residues. On the other hand, polar solvation (ΔG _bind, SolvGB \approx +20.51 kcal/mol) and Coulombic interactions (ΔG _bind, Coulomb \approx +12.13 kcal/mol) are both bad, showing the desolvation penalty that happens when polar groups are stuck in a mostly apolar cavity with little

charge-charge stabilization. Because MM-GBSA divides its effect between solvation and Coulombic parts, the small but helpful hydrogen-bond contribution (ΔG_{-} bind, Hbond \approx -1.08 kcal/mol) probably doesn't show how important the VAL882 interactions are in a qualitative way. Still, the almost linear shape (172.5° for one bond) shows that these interactions have enthalpic benefits that are somewhat canceled out by desolvation, resulting in a small net value in the analysis. The small positive "covalent" term (+3.56 kcal/mol) shows that 11325 does not have to pay a lot of conformational cost to take on its bound shape. This means that constrained internal strain during binding is not very high. The energy pattern tells a consistent story: (i) The ligand's shape and polar surface area fit well with a hydrophobic kinase pocket, which improves dispersion (strong negative van der Waals interactions) and nonpolar entrapment (negative lipophilicity); (ii) only two highquality hinge hydrogen bonds are formed, which is not enough to completely counteract the desolvation penalty of all polar groups (positive Solvation Gibbs free energy and Coulombic interactions), but the overall result is still very good; and (iii) the docking score, which takes into account pose quality, shape complementarity, and hydrogen bond geometry, matches the MM-GBSA analysis of dispersion-driven stabilization enhanced by specific hinge recognition. From the perspective of medicinal chemistry, the interaction map suggests several logical improvements: enhancing the hinge binding (for example, by altering pKa or pointing an extra heteroatom in the direction of the VAL882 backbone NH/CO) could make the polar terms less harmful by replacing desolvation costs with stronger and more numerous protein-ligand hydrogen bonds; or extending hydrophobic substituents into accessible lipophilic subpockets close to TRP812/TYR867 could further exploit the pocket's dispersion potential, enhancing the already substantial van der Waals and lipophilic terms without appreciably increasing desolvation penalties. But you have to be careful not to add hidden unsatisfied polar atoms, which could make SolvGB worse and maybe even change the shape of the molecule; on the other hand, too much polarity could weaken the hydrophobic driving force that keeps affinity strong. Small para/ortho substitutions that keep the planarity may be better than big, branched groups that could get in the way of the side chains of ILE879/ILE881, as shown by the narrow hydrophobic distances (3.2–3.8 Å).

Finally, the two identified VAL882 hydrogen bonds, with their ideal geometry, offer a promising selectivity mechanism: keeping their vectors while modifying the periphery to align with the hydrophobic edge of TYR867 or interact with the face of TRP812 (π – π or edge–face interactions with aromatic structures) may increase potency without requiring additional desolvation costs. The alignment of the structure-based docking model (hydrophobic packing plus two hinge hydrogen bonds) with the energy-based MM-GBSA decomposition (significantly negative van der Waals and lipophilic contributions, moderately favorable hydrogen bonds, offset by positive solvation and Coulombic terms) gives a clear mechanistic explanation for why 11325 can bind to PI3K and a clear guide for how to improve affinity and selectivity (see Supplementary Material for MMGBSA results).

3.2. MD Simulation Analysis

3.2.1. RMSD

We ran a molecular dynamics (MD) simulation of ligand 11325 with the Phosphoinositide 3-kinase (PI3K) receptor (PDB ID: 1e7u) for over 100 ns. The RMSD analysis gives us important information about how stable and flexible the complex is. The RMSD figure shows that the protein backbone ($C\alpha$ RMSD) goes through a phase of equilibration that lasts about 15 ns before settling down between 2.2 and 2.8 Å. This means that the protein's structure stayed the same during the simulation. In the first 10 ns, the ligand RMSD (aligned with the protein backbone) changed a lot. This suggests that the ligand was getting used to its new place in the binding pocket. After about 15 ns, the ligand RMSD stayed

between 1.2 and 2.0 Å, with some temporary changes that peaked at about 3.5 Å at the end of the simulation. This suggests that the ligand stayed in the pocket but was able to change shape, likely because it interacted with the moving side chains in the active site. The steady RMSD trend shows that ligand 11325 stayed attached to the PI3K binding cleft the whole time during the 100 ns trajectory. These dynamic data raise the docking score from -8.558 kcal/mol, which before indicated a strong binding affinity (see Figure 2).

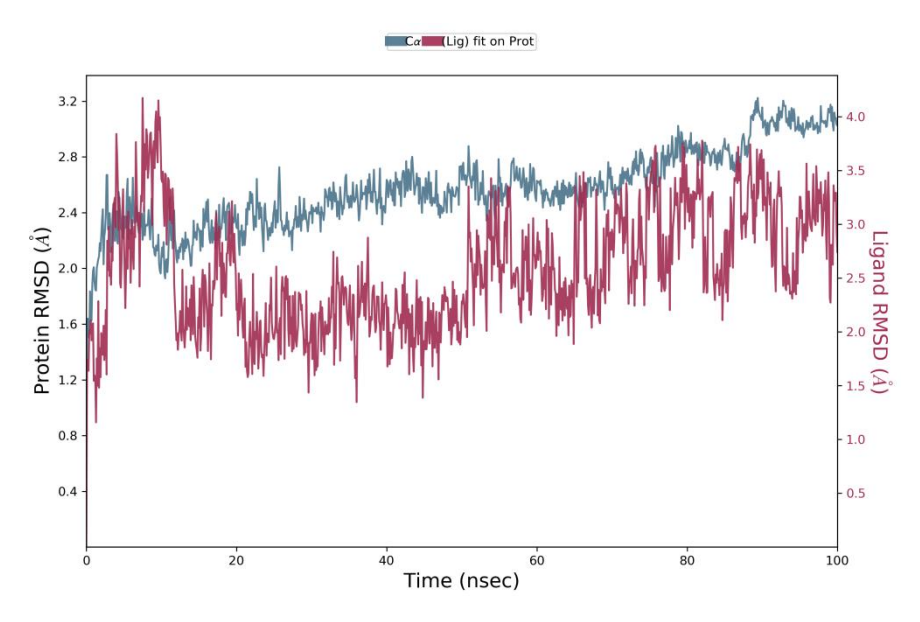


Figure 2. Presentation of Protein: Phosphoinositide 3-kinase (PI3K) receptor (PDB ID: 1e7u) and ligand 11325 RMSD variations during 100 ns molecular dynamics simulation.

The docking interaction profile showed that the residues TRP812, ILE831, TYR867, ILE879, and ILE881 had strong hydrophobic contacts with each other. It also showed that VAL882 had two strong hydrogen bonds with each other (bond lengths of about 1.85–1.98 Å, which is perfect for stability). The steady RMSD of the ligand throughout the simulation shows that these interactions were stable. Hydrogen bonds helped keep the ligand in place, and hydrophobic residues made sure that the pocket was full and that the ligand didn't get too much solvent. The ligand RMSD going above 3 Å every now and then is probably because it moved around in the binding site for a short time, not because it broke apart. This is consistent with the inherent flexibility of hydrophobic side chains. The results of docking and molecular dynamics together show that ligand 11325 binds strongly and favorably within the PI3K active site. This is backed up by strong hydrogen bonding and hydrophobic interactions, which make it a good candidate for further optimization in drug development that targets PI3K. In kinase drug development, similar methods that combine docking and molecular dynamics have been widely used to test the stability of ligands and the compatibility of receptors and ligands.

3.2.2. RMSF

The root-mean-square fluctuation (RMSF) profiles show how much each residue moves away from its average location during the trajectory. The $C\alpha$ RMSF trace you gave me (100 ns; y-axis in Å, x-axis as residue index) shows how flexible the PI3K receptor is when ligand 11325 is there. The protein doesn't move much at all, only about 0.6 to 1.4 Å across large areas. There are clear peaks that go above 3 Å and up to about 5.5 Å in some loop and terminal parts (for example, 110–120, ~240–260, ~300–320, and a cluster at 750–810). These spikes show that there are loops and chain ends that are open to the solvent, but they don't mean that the ligand is unstable by itself. The residues that make up the

docking-defined binding pocket, TRP812, ILE831, TYR867, ILE879, ILE881, and VAL882, are all in an area with an average RMSF that is within the range of 0.8–1.6 Å. There is only a small rise at about 810, which means that there is a mobility loop close to Trp812 (see Figure 3).

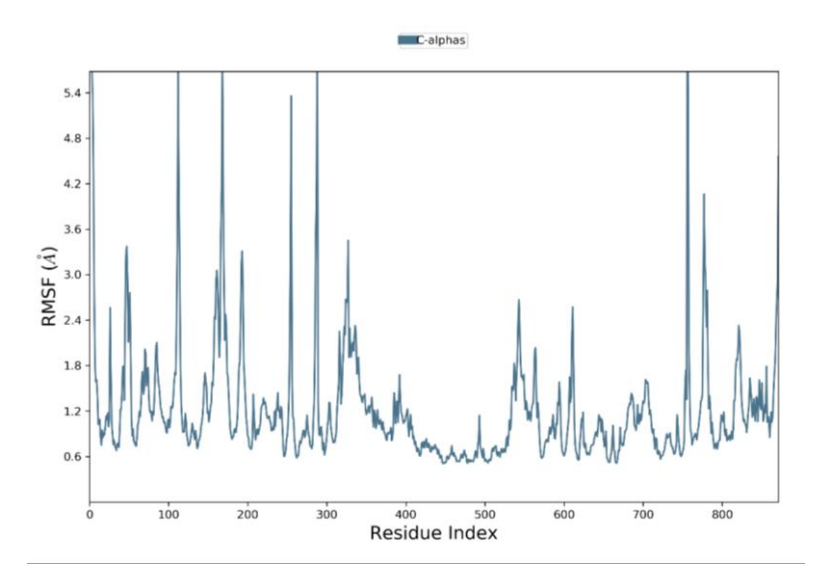


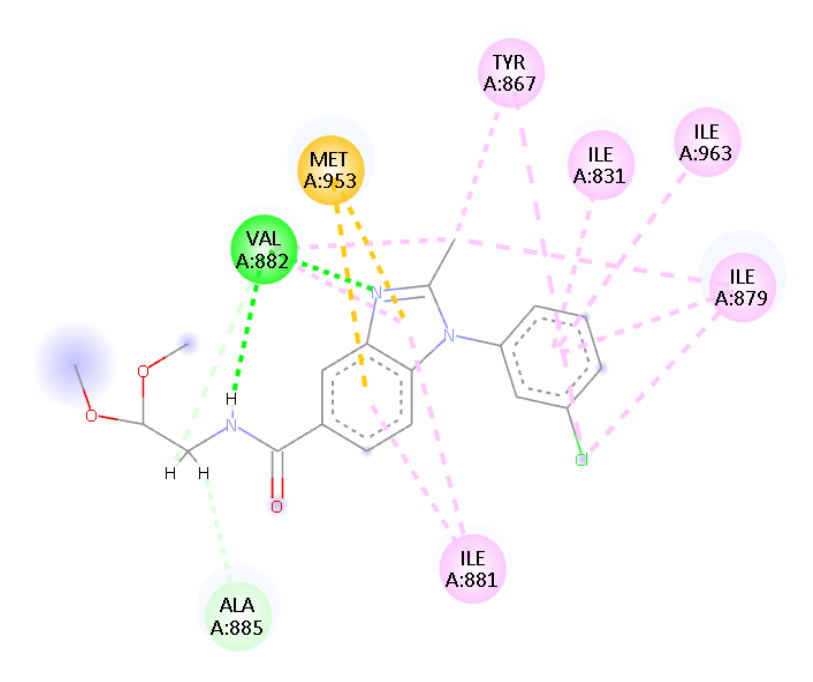
Figure 3. Root Mean Square Fluctuation (RMSF) profile of $C\alpha$ atoms across protein residues.

The residues Tyr867, Ile879, Ile881, and Val882 in the downstream pocket don't change much, which means that the active site is well-structured. The docking conformation (score–8.558 kcal/mol) is supported by this pattern. In this conformation, hydrophobic residues (TRP812/ILE831/TYR867/ILE879/ILE881) surround the ligand, and two short hydrogen bonds to VAL882 (with H-bond donor-acceptor distances of about 1.85-1.98 Å and angles of about 145–172°) act as stabilizing anchors. The low to moderate RMSF for Val882 and nearby residues is what we would expect if H-bonding were going on in a hidden kinase pocket. The few high spikes around the pocket (especially at ~780-810) probably show how the peripheral loops move when they breathe. These movements might change the volume of the pocket for a short time and explain the changes in ligand RMSD that happen near the end of the journey without breaking the bond. The RMSF map shows that the area around the binding site is hard, and the area around it is flexible. This is something that lipid/ATP-site kinases often have in common. This finding supports the MD-derived stability of ligand 11325. The anchor residue (Val882) and the hydrophobic cage residues stay pretty stable for 100 ns, which matches the good docking energy and interaction pattern.

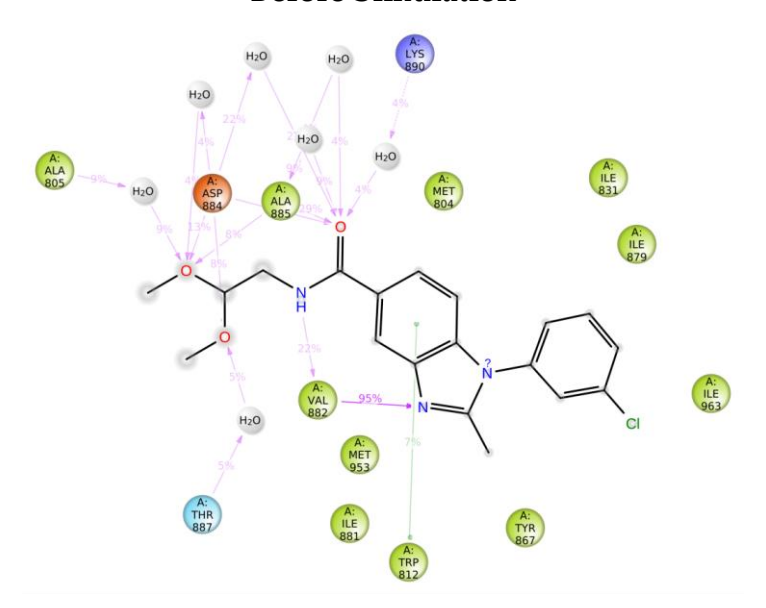
3.2.3. Analysis of 11325 Phosphoinositide 3-Kinase (PI3K; PDB: 1e7u) Receptor Interactions Before and After MD Simulation

Ligand 11325 was placed in the ATP-binding pocket of PI3K (PDB: 1E7U; see structure at RCSB: https://www.rcsb.org/structure/1E7U). Its pre-MD posture showed that it fit tightly (docking score -8.558 kcal/mol), thanks to a combination of hydrogen bonding and hydrophobic interactions. The ligand is held to the hinge region residue Val882 by two direct hydrogen bonds. The first is a short donor interaction (H-A = 1.85 Å; D-A = 2.75 Å; \angle = 145.6°) between a ligand amide nitrogen (Nam, atom 14221) and a carbonyl oxygen on the protein (O2, atom 10950). The second is a nearly linear interaction (H-A = 1.98 Å; D-A = 2.98 Å; \angle = 172.5°) between an aromatic nitrogen on the ligand (Nar, atom 14212) and a protein acceptor (atom 10947). Trp812 (3.40 Å), Ile831 (3.79 Å), Tyr867 (3.23 Å), Ile879 (3.60 Å), and Ile881 (3.69 Å) make up the hydrophobic shell around these polar

anchors. This is how PI3K inhibitors usually attach to hinges. The 2D contact map shows that this binding motif is still there and has been improved after molecular dynamics. The hinge hydrogen bond to Val882 is still strong (95% occupancy), which shows that the original hydrogen-bond geometry was almost perfect and is still the main reason why the pose stays stable. A reduced aromatic interaction with Trp812 is observed sporadically (7%), indicating edge-to-face π interactions as the indole side chain fluctuates during the process (see Figure 4).



Before Simulation



After 100ns Simulation

Figure 4. Portrayal of 2D interactions of Ligand 11325 with Phosphoinositide 3-kinase (PI3K) receptor (PDB ID: 1e7u) before and after simulation.

The hydrophobic cage that repels water is still mostly whole. The two ligand rings and the chloro-phenyl terminal still have Ile831, Ile879, Ile881, and Tyr867 in them. But

Met804 and Met953 are close enough to each other that they are temporarily interacting with each other through van der Waals forces. This supports the ligand core's ongoing desolvation. MD makes a network of structured water next to the amide/ester area that is open to the solvent. Water molecules connect the ligand carbonyl/ether oxygens to Asp884 and Ala885 (4–29% of the time), then move toward Lys890 through more water molecules (4%), and sometimes interact with Thr887 (5%). Water interactions explain why only one of the two initial direct Val882 hydrogen bonds is mostly occupied. Instead of two lasting direct connections, rearranging the local area makes one stable hinge bond and one dynamic hydrogen bond/solvent relay. In short, MD helps 11325 take on a stable shape with hinges that keep hydrophobic interactions, a strong Val882 hydrogen bond, extra π -stacking with Trp812, and a flexible water network around Asp884/Ala885. This network could be used to make it stronger or more selective, for example, by making polar changes to stabilize the water bridge or lipophilic changes to make it interact better with Ile879/Ile881.

4. ADME Study

A comparative ADMET analysis of the four top-docked compounds (11393, 4153, 11345, and 4162) reveals that compound 11325 possesses distinct advantages that render it an optimal candidate for PI3K inhibition. The best docking score for compound 11393 is -8.688 kcal/mol, which is a little bit better than the score for compound 11325, which is -8.55 kcal/mol. But the way it looks and works isn't quite right. Compound 11393 is druglike and has a molecular weight of 373.42 Da. However, its high lipophilicity (consensus logP = 4.43) and low polar surface area (TPSA = 46.9 Å²) suggest that it may be too permeable and may have trouble dissolving. It also doesn't meet two of the lead-likeness criteria and one of the Lipinski criteria, which makes it less likely to be a good candidate for a full drug. The docking score for compound 4153 is -8.663 kcal/mol, which means it is very close to being the most drug-like. The weight of its molecules is higher (454.75 Da). It doesn't meet two of Lipinski's criteria for lead-likeness, and it has a high lipophilicity (logP = 4.99), which means it is less likely to be chemically tractable and easy to take by mouth. Compound 11345 is a little heavier (399.48 Da) and has three hydrogen bond acceptors instead of four, like 11325. It doesn't break any of Lipinski's rules. It has a lipophilic profile that is too high, with a logP of 4.50. This could make it hard for the body to dissolve and stay stable. Compound 4162 has a great docking score (-8.339 kcal/mol), but it has the same problems because it is very lipophilic (logP = 4.75) and it doesn't meet one of Lipinski's criteria. 11325 is one of a kind because it has a balanced consensus logP of 3.13. This means that it has the right amount of lipophilic and hydrophilic properties to let enough molecules pass through the membrane while still being able to dissolve. It has a TPSA of 65.38 Å², which is more than the others but still less than 140 Å². This helps the intestines absorb the medicine and not too much through the CNS, which is what you want for an anticancer target like PI3K. It is okay to keep working on 11325 because it only has one lead-likeness violation and no Lipinski violations. It also has a low score of 2.68 for how easy it is to make synthetic. People believe that the intestines will better absorb all five chemicals and that they will be able to cross the blood-brain barrier more easily. But compound 11325 is the best because it has a better balance between polarity and lipophilicity. This means that it is less likely to cause off-target toxicity and poor solubility. None of the compounds had PAINS warnings, but 11325 does have a small Brenk alert. This could be because it has a chloro group, which is common and easy to work with in ki-nase inhibitors. It is possible that all of the drugs will stop different CYP isoforms from working, which could be bad. But 11325 might be more stable in the body and less likely to be quickly removed or cause off-target metabolic inhibition because it is less lipophilic than its analogs. In conclusion, 11325 may not have the highest docking score, but it has the best mix of drug-like physical and chemical properties, no major rule violations,

moderate flexibility (7 rotatable bonds), a good balance between solubility and permeability, and is easy to make. This strongly supports its claim to be the best hit molecule for blocking PI3K (see ADME Results in the Supplementary Material Table S1).

5. PCA & Free Energy Landscape Study

When you put together docking analysis with PCA and Free Energy Landscape (FEL) data, you get a complete picture of how stable ligand–protein interactions are and how they change over time during molecular simulation. The first docking of ligand molecule 11325 with the PI3K receptor (pdb: 1e7u) resulted in a favorable binding score of -8.558 kcal/mol, indicating a strong affinity and the possibility of stable complex formation. There are a lot of hydrophobic contacts that make up the docking interactions, mostly with residues TRP812, ILE831, TYR867, ILE879, and ILE881. These contacts create a pocket that keeps the ligand in place. We also found strong hydrogen bonds with VAL882. These bonds had short donor–acceptor distances (1.85–1.98 Å) and bond angles that were almost straight (145–172°). This means that the hydrogen bonding is strong and directed, which keeps the ligand stable in the active site. After the simulation, the PCA and FEL analyses check the static docking predictions dynamically. The PCA projections show clear conformational clusters, which means that the protein-ligand complex moves through a number of metastable states during the simulation, even though the docking connections are strong (see Figure 5).

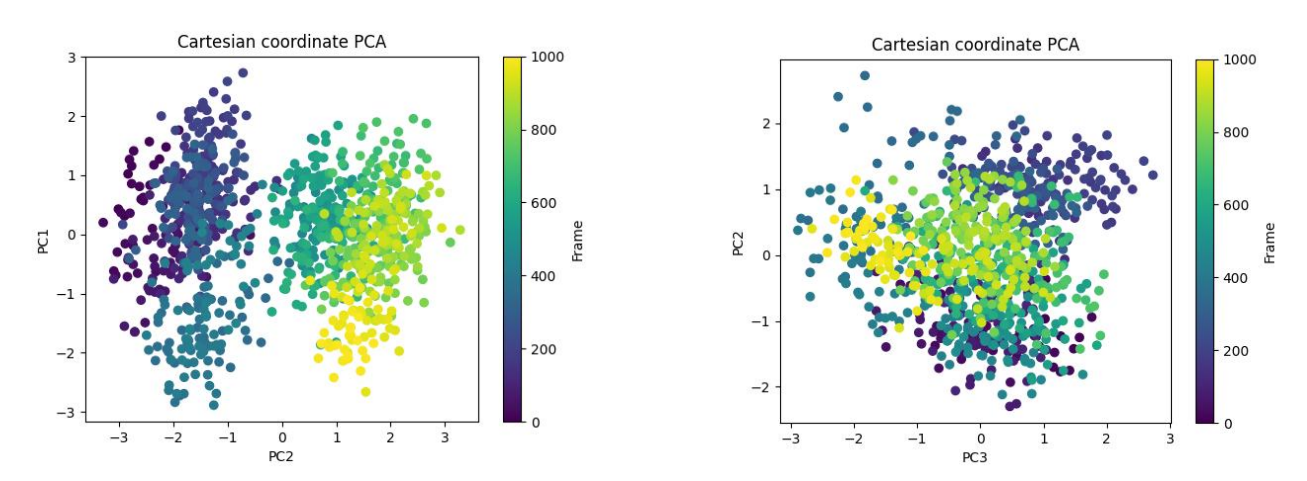


Figure 5. Display of PCA projection of molecular dynamics trajectories highlighting conformational clustering across frames.

The two main basins in the PC1–PC2 space show the conformational equilibrium of the protein–ligand system. This means that the binding pocket and ligand orientation have shifted slightly, but the overall stability remains unchanged. The FEL data back up this moving picture by showing a deep free energy basin with an RMSD of about 0.20–0.30 nm and an RG of about 2.56–2.59 nm. This indicates that the system predominantly investigates a stable, restricted conformational ensemble. The ligand's hydrophobic interactions create a low-energy environment that encourages compactness (as shown by the RG), while stable hydrogen bonds help to reduce structural errors (as shown by the RMSD stability). The docking data and free energy landscape show that the ligand-receptor complex is not only firmly attached during the static docking phase, but it also stays stable in dynamic conditions that mimic real life. The free energy funnel demonstrates that the binding conformation is thermodynamically advantageous. The shallow neighboring minima in the FEL indicate that the molecule is capable of conformational change, which may be significant for the regulation of PI3K or for ligand adaptation (see Figure 6).

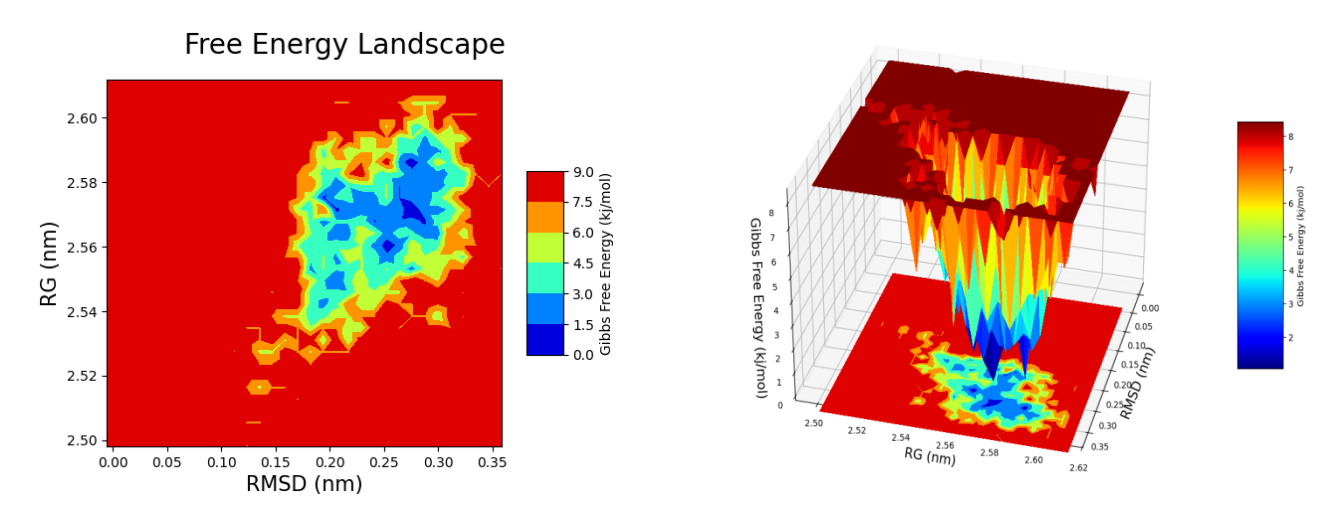


Figure 6. Presentation of 2D and 3D Gibbs free energy surfaces highlight stable structural basins and transitions in the protein ensemble.

The combination of docking (binding affinity and interaction fingerprint), PCA (conformational partitioning), and FEL (thermodynamic stability) leads to a clear conclusion: ligand 11325 creates a strong interaction network in the PI3K binding site, undergoes limited but functionally important conformational changes, and mostly stays in a stable free energy basin, making it a strong candidate for a PI3K inhibitor.

6. Conclusions

This study finds that compound 11325 is a good candidate for selective PI3K inhibition. It has a unique set of physicochemical, pharmacokinetic, and stability properties that set it apart from other similar compounds found through structure-based docking. Instead of just focusing on improving docking scores, this study uses docking, MM-GBSA energy decomposition, molecular dynamics, free energy landscape analysis, and ADMET profiling to give a full mechanistic story and make sure it is useful in the real world. The docking results showed that 11325 has a strong binding affinity of -8.558 kcal/mol because it has a good mix of van der Waals interactions, lipophilic packing, and hinge-directed hydrogen bonding with Val882. These three things work together to keep the ligand in a specific kinase-recognition motif. The molecular dynamics trajectory showed that these connections are permanent because the RMSD/RMSF values stayed the same and the hydrophobic cage made by TRP812, ILE831, TYR867, ILE879, and ILE881 didn't break very often. This persistence shows that the ligand can handle changes in shape. Principal component analysis (PCA) shows that the ligand can only cluster in certain shapes, and free energy landscape (FEL) data shows that there is a deep, stable energy basin that suggests thermodynamic favourability. It's important to note that 11325 had a drug-like profile that was better than that of other high-scoring analogs. It had a lipophilicity of 3.13, a polarity of 65.38 Å², and a synthetic accessibility of 2.68. There were no Lipinski violations and no major structural alerts. All of this makes it more likely that the body will absorb it, that it will dissolve better, and that it will have a lower risk of off-target liabilities. This combined validation framework shows that compound 11325 is more than just a "virtual hit"; it is also a carefully chosen scaffold with clinical potential. It also offers a novel methodological framework for kinase inhibitor discovery by showing that real lead identification needs the combination of binding affinity, stability dynamics, thermodynamic landscapes, and ADMET rationality, rather than just single-parameter optimizations. Because of this, compound 11325 is known to be a strong and stable PI3K binder, making it a promising candidate for therapy that needs more testing in animals before it can be used in humans. Its hinge-centric selectivity and hydrophobic optimization give it a mechanistic edge in the search for new anticancer drugs that target PI3K.

Supplementary Materials:

Author Contributions: M.B. and R.D.J., conceived and supervised this study. R.D.J. and H.B. accomplished drafting and review. M.B., and P.N.K. Collected and curated the data. R.D.J. and P.V.B. processed the data and analysed the results. All authors have read and agreed to the published version of the manuscript.

Funding:

Institutional Review Board Statement:

Informed Consent Statement:

Data Availability Statement:

Acknowledgments: Authors are thankful to Hon. Shri Yogendraji Gode Sir, President IBBS'S Buldana, Rajendra Gode Institute of Pharmacy, Amravati for extended support during entire course of research work.

Conflicts of Interest:

References

- 1. Murga, C.; Fukuhara, S.; Gutkind, J.S. A Novel Role for Phosphatidylinositol 3-Kinase β in Signaling from G Protein-coupled Receptors to Akt. *J. Biol. Chem.* **2000**, 275, 12069–12073. https://doi.org/10.1074/jbc.275.16.12069.
- 2. Houslay, D.M.; Anderson, K.E.; Chessa, T.; Kulkarni, S.; Fritsch, R.; Downward, J.; Backer, J.M.; Stephens, L.R.; Hawkins, P.T. Coincident signals from GPCRs and receptor tyrosine kinases are uniquely transduced by PI3Kβ in myeloid cells. *Sci. Signal.* **2016**, *9*, ra82. https://doi.org/10.1126/scisignal.aae0453.
- 3. Rathinaswamy, M.K.; Burke, J.E. Class I phosphoinositide 3-kinase (PI3K) regulatory subunits and their roles in signaling and disease. *Adv. Biol. Regul.* **2020**, *75*, 100657. https://doi.org/10.1016/j.jbior.2019.100657.
- 4. Schiebel, C.S.; Mazeti, S.S.S.; Gois, M.B.; Maria-Ferreira, D. Editorial: Gastrointestinal damage and metabolic disorders. *Front. Physiol.* **2025**, *16*, 1648739. https://doi.org/10.3389/fphys.2025.1648739.
- 5. Shaikat, A.H.; Azad, S.M.A.K.; Tamim, M.A.R.; Ullah, M.S.; Amin, M.N.; Sabbir, M.K.; Tarun, M.T.I.; Mostaq, M.S.; Sabrin, S.; Mahmud, M.Z.; et al. Investigating hypoxia-inducible factor signaling in cancer: Mechanisms, clinical impli-cations, targeted therapeutic strategies, and resistance. *Cancer Pathog. Ther.* **2025**.
- 6. Kim, B.-S.; Kim, B.; Yoon, S.; Park, W.; Bae, S.-J.; Joo, J.; Kim, W.; Ha, K.-T. Warburg-like Metabolic Reprogramming in Endometriosis: From Molecular Mechanisms to Therapeutic Approaches. *Pharmaceuticals* **2025**, *18*, 813.
- 7. Cancer Genome Atlas Network. Comprehensive molecular portraits of human breast tumours. Nature 2012, 490, 61–70.
- 8. Samuels, Y.; Wang, Z.; Bardelli, A.; Silliman, N.; Ptak, J.; Szabo, S.; Yan, H.; Gazdar, A.; Powell, S.M.; Riggins, G.J.; et al. High Frequency of Mutations of the *PIK3CA* Gene in Human Cancers. *Science* 2004, 304, 554. https://doi.org/10.1126/science.1096502.
- 9. Mayer, I.A.; Arteaga, C.L. The PI3K/AKT Pathway as a Target for Cancer Treatment. *Annu. Rev. Med.* 2016, 67, 11–28. https://doi.org/10.1146/annurev-med-062913-051343.
- 10. Okkenhaug, K.; Vanhaesebroeck, B. PI3K in lymphocyte development, differentiation and activation. *Nat. Rev. Immunol.* **2003**, 3, 317–330. https://doi.org/10.1038/nri1056.
- 11. Lannutti, B.J.; Meadows, S.A.; Herman, S.E.M.; Kashishian, A.; Steiner, B.; Johnson, A.J.; Byrd, J.C.; Tyner, J.W.; Loriaux, M.M.; Deininger, M.; et al. CAL-101, a p110δ selective phosphatidylinositol-3-kinase inhibitor for the treatment of B-cell malignancies, inhibits PI3K signaling and cellular viability. *Blood* **2011**, *117*, 591–594. https://doi.org/10.1182/blood-2010-03-275305.
- 12. Apostolidis, J.; Mokhtar, N.; Al Omari, R.; Darweesh, M.; Al Hashmi, H. Follicular lymphoma: Update on management and emerging therapies at the dawn of the new decade. *Hematol. Oncol.* **2020**, *38*, 213–222.
- 13. Yu, M.; Chen, J.; Xu, Z.; Yang, B.; He, Q.; Luo, P.; Yan, H.; Yang, X. Development and safety of PI3K inhibitors in cancer. *Arch. Toxicol.* **2023**, *97*, 635–650. https://doi.org/10.1007/s00204-023-03440-4.

- 14. Lin, X.; Zhang, Y.; Huang, H.; Zhuang, W.; Wu, L. Post-marketing safety concern of PI3K inhibitors in the cancer therapies: An 8-year disproportionality analysis from the FDA Adverse Event Reporting System. *Expert Opin. Drug Saf.* **2024**, 24, 925–936. https://doi.org/10.1080/14740338.2024.2387317.
- 15. Vangapandu, H.V.; Jain, N.; Gandhi, V. Duvelisib: A phosphoinositide-3 kinase δ/γ inhibitor for chronic lymphocytic leu-kemia. *Expert Opin. Investig. Drugs* **2017**, *26*, 625–632.
- 16. Shi, M.; Chen, T.; Wei, S.; Zhao, C.; Zhang, X.; Li, X.; Tang, X.; Liu, Y.; Yang, Z.; Chen, L. Molecular Docking, Molecular Dynamics Simulations, and Free Energy Calculation Insights into the Binding Mechanism between VS-4718 and Focal Adhesion Kinase. *ACS Omega* 2022, 7, 32442–32456. https://doi.org/10.1021/acsomega.2c03951.
- 17. Sadybekov, A.V.; Katritch, V. Computational approaches streamlining drug discovery. *Nature* **2023**, *616*, 673–685. https://doi.org/10.1038/s41586-023-05905-z.
- 18. Gajulapalli, V.P.R. Development of Kinase-Centric Drugs: A Computational Perspective. *ChemMedChem* **2023**, *18*, e202200693. https://doi.org/10.1002/cmdc.202200693.
- 19. Kato, K.; Nakayoshi, T.; Kurimoto, E.; Oda, A. Molecular dynamics simulations for the protein–ligand complex structures obtained by computational docking studies using implicit or explicit solvents. *Chem. Phys. Lett.* **2021**, 781, 139022. https://doi.org/10.1016/j.cplett.2021.139022.
- 20. Forouzesh, N.; Onufriev, A.V. 2020.
- 21. Salmaso, V.; Moro, S. Bridging Molecular Docking to Molecular Dynamics in Exploring Ligand-Protein Recognition Process: An Overview. *Front. Pharmacol.* **2018**, *9*, 923. https://doi.org/10.3389/fphar.2018.00923.
- 22. Halder, D.; Mukherjee, S.; Jeyaprakash, R.S. Exploring target selectivity in designing and identifying PI3Kα inhibitors for triple negative breast cancer with fragment-based and bioisosteric replacement approach. *Sci. Rep.* **2025**, *15*, 1890. https://doi.org/10.1038/s41598-024-83030-1.
- 23. Zhang, M.; Jang, H.; Nussinov, R. PI3K inhibitors: Review and new strategies. *Chem. Sci.* **2020**, *11*, 5855–5865. https://doi.org/10.1039/d0sc01676d.
- 24. Jia, W.; Luo, S.; Zhao, W.; Xu, W.; Zhong, Y.; Kong, D. Discovery of Novel PI3Kδ Inhibitors Based on the p110δ Crystal Structure. *Molecules* **2022**, 27, 6211.
- 25. Tang, S.-L.; Sumitra, M.R.; Kuo, Y.-C.; Hsu, H.-L.; Ansar, M.; Huang, S.-L.; Lee, S.-Y.; Wang, H.-J.; Lawal, B.; Wu, A.T.; et al. Computer-aided drug discovery of a dual-target inhibitor for ovarian cancer: Therapeutic intervention targeting CDK1/TTK signaling pathway and structural insights in the NCI-60. *Comput. Biol. Med.* 2025, 193, 110445. https://doi.org/10.1016/j.compbiomed.2025.110445.
- 26. Ketcham, J.M.; Harwood, S.J.; Aranda, R.; Aloiau, A.N.; Bobek, B.M.; Briere, D.M.; Burns, A.C.; Haatveit, K.C.; Calinisan, A.; Clarine, J.; et al. Discovery of Pyridopyrimidinones that Selectively Inhibit the H1047R PI3Kα Mutant Protein. *J. Med. Chem.* **2024**, *67*, 4936–4949. https://doi.org/10.1021/acs.jmedchem.4c00078.
- 27. Drew, S.L.; Thomas-Tran, R.; Beatty, J.W.; Fournier, J.; Lawson, K.V.; Miles, D.H.; Mata, G.; Sharif, E.U.; Yan, X.; Mailyan, A.K.; et al. Discovery of Potent and Selective PI3Kγ Inhibitors. *J. Med. Chem.* **2020**, *63*, 11235–11257.
- 28. Zhu, J.; Li, K.; Xu, L.; Cai, Y.; Chen, Y.; Zhao, X.; Li, H.; Huang, G.; Jin, J. Discovery of novel selective PI3Kγ inhibitors through combining machine learning-based virtual screening with multiple protein structures and bio-evaluation. *J. Adv. Res.* **2022**, *36*, 1–13. https://doi.org/10.1016/j.jare.2021.04.007.
- 29. Mishra, R.; Patel, H.; Alanazi, S.; Kilroy, M.K.; Garrett, J.T. PI3K Inhibitors in Cancer: Clinical Implications and Adverse Effects. *Int. J. Mol. Sci.* **2021**, 22, 3464. https://doi.org/10.3390/ijms22073464.
- 30. Nunnery, S.E.; Mayer, I.A. Management of toxicity to isoform α-specific PI3K inhibitors. Ann. Oncol. 2019, 30, x21–x26.
- 31. A. Sabbah, D.; Hu, J.; A. Zhong, H., Advances in the Development of Class I Phosphoinositide 3-Kinase (PI3K) Inhibitors. *Curr. Top. Med. Chem.* **2016**, *16*, 1413–1426.
- 32. Sabbah, D.A.; Vennerstrom, J.L.; Zhong, H. Docking Studies on Isoform-Specific Inhibition of Phosphoinositide-3-Kinases. *J. Chem. Inf. Model.* **2010**, *50*, 1887–1898. https://doi.org/10.1021/ci1002679.
- 33. Morris, G.M.; Huey, R.; Olson, A.J. Using AutoDock for Ligand-Receptor Docking. Curr. Protoc. Bioinform. 2008, 24, 8-14.
- 34. Morris, G.M.; Huey, R.; Lindstrom, W.; Sanner, M.F.; Belew, R.K.; Goodsell, D.S.; Olson, A.J. AutoDock4 and AutoDockTools4: Automated docking with selective receptor flexibility. *J. Comput. Chem.* **2009**, *30*, 2785–2791. https://doi.org/10.1002/jcc.21256.
- 35. Walker, E.H.; Perisic, O.; Ried, C.; Stephens, L.; Williams, R.L. 2000.
- 36. Halgren, T.A. Merck molecular force field. I. Basis, form, scope, parameterization, and performance of MMFF94. *J. Comput.* Chemistry **1996**, *17*, 490–519.

- 37. Laskowski, R.A.; Swindells, M.B. LigPlot+: Multiple ligand–protein interaction diagrams for drug discovery. *J. Chem. Inf. Model.* **2011**, *51*, 2778–2786. https://doi.org/10.1021/ci200227u.
- 38. Jorgensen, W.L.; Maxwell, D.S.; Tirado-Rives, J. Development and Testing of the OPLS All-Atom Force Field on Conformational Energetics and Properties of Organic Liquids. *J. Am. Chem. Soc.* **1996**, *118*, 11225–11236. https://doi.org/10.1021/ja9621760.
- 39. Hoover, W.G. Canonical dynamics: Equilibrium phase-space distributions. *Phys. Rev. A* **1985**, *31*, 1695–1697. https://doi.org/10.1103/physreva.31.1695.
- 40. Nosé, S. A molecular dynamics method for simulations in the canonical ensemble. Mol. Phys. 2006, 52, 255–268.
- 41. Bowers, K.J.; Sacerdoti, F.D.; Salmon, J.K.; Shan, Y.; Shaw, D.E.; Chow, E.; Xu, H.; Dror, R.O.; Eastwood, M.P.; Gregersen, B.A.; et al. Molecular dynamics---Scalable algorithms for molecular dynamics simulations on commodity clusters. In Proceedings of the 2006 ACM/IEEE Conference on SUPERCOMPUTING—SC '06, Tampa, FL, USA, 11–17 November 2006.
- 42. Jorgensen, W.L.; Chandrasekhar, J.; Madura, J.D.; Impey, R.W.; Klein, M.L. Comparison of simple potential functions for simulating liquid water. *J. Chem. Phys.* **1983**, *79*, 926–935. https://doi.org/10.1063/1.445869.
- 43. Kumar, S.; Rosenberg, J.M.; Bouzida, D.; Swendsen, R.H.; Kollman, P.A. THE weighted histogram analysis method for free-energy calculations on biomolecules. I. The method. *J. Comput. Chem.* **2004**, *13*, 1011–1021.
- 44. Grant, B.J.; Rodrigues, A.P.; ElSawy, K.M.; McCammon, J.A.; Caves, L.S. Bio3d: An R package for the comparative analysis of protein structures. *Bioinformatics* **2006**, 22, 2695–2696. https://doi.org/10.1093/bioinformatics/btl461.
- 45. Hollingsworth, S.A.; Dror, R.O. Molecular Dynamics Simulation for All. Neuron 2018, 99, 1129-1143.
- 46. Cantley, L.C. The Phosphoinositide 3-Kinase Pathway. Science 2002, 296, 1655–1657.
- 47. Wang, E.; Sun, H.; Wang, J.; Wang, Z.; Liu, H.; Zhang, J.Z.H.; Hou, T. End-Point Binding Free Energy Calculation with MM/PBSA and MM/GBSA: Strategies and Applications in Drug Design. *Chem. Rev.* **2019**, *119*, 9478–9508. https://doi.org/10.1021/acs.chemrev.9b00055.
- 48. Genheden, S.; Ryde, U. The MM/PBSA and MM/GBSA methods to estimate ligand-binding affinities. *Expert Opin. Drug Discov.* **2015**, *10*, 449–461. https://doi.org/10.1517/17460441.2015.1032936.
- 49. David, C.C.; Jacobs, D.J. Principal Component Analysis: A Method for Determining the Essential Dynamics of Proteins. In *Protein Dynamics*; Humana Press: Totowa, NJ, USA, 2014; pp. 193–226.
- 50. Maisuradze, G.G.; Liwo, A.; Scheraga, H.A. Principal Component Analysis for Protein Folding Dynamics. *J. Mol. Biol.* **2009**, *385*, 312–329. https://doi.org/10.1016/j.jmb.2008.10.018.
- 51. Abraham, M.J.; Murtola, T.; Schulz, R.; Páll, S.; Smith, J.C.; Hess, B.; Lindahl, E. GROMACS: High performance molecular simulations through multi-level parallelism from laptops to supercomputers. *SoftwareX* **2015**, *1*–2, 19–25. https://doi.org/10.1016/j.softx.2015.06.001.
- 52. Amadei, A.; Linssen, A.B.M.; Berendsen, H.J.C. Essential dynamics of proteins. *Proteins Struct. Funct. Bioinform.* **2004**, *17*, 412–425.
- 53. Akama, T.; Virtucio, C.; Dong, C.; Kimura, R.; Zhang, Y.-K.; Nieman, J.A.; Sharma, R.; Lu, X.; Sales, M.; Singh, R.; et al. Structure–activity relationships of 6-(aminomethylphenoxy)-benzoxaborole derivatives as anti-inflammatory agent. *Bioorg. Med. Chem. Lett.* 2013, 23, 1680–1683. https://doi.org/10.1016/j.bmcl.2013.01.072.

Disclaimer/Publisher's Note: The statements, opinions and data contained in all publications are solely those of the individual author(s) and contributor(s) and not of MDPI and/or the editor(s). MDPI and/or the editor(s) disclaim responsibility for any injury to people or property resulting from any ideas, methods, instructions or products referred to in the content.